A generalized dynamical thermostatting technique

Brian B. Laird

Department of Chemistry and Kansas Institute for Theoretical and Computational Science
University of Kansas
Lawrence, Kansas 66045, USA

Benedict J. Leimkuhler

Department of Mathematics and Computer Science University of Leicester
Leicester, LE1 7RH, UK

(Dated: January 15, 2003)

Abstract

We demonstrate that the Nosé method for constant-temperature molecular-dynamics simulation [Mol. Phys. **52**, 255 (1984)] can be substantially generalized by the addition of auxilliary variables to encompass an infinite variety of Hamiltonian thermostats. Such themostats can be used to enhance ergodicity in systems, such as the 1-d harmonic oscillator or certain molecular systems, for which the standard Nosé-Hoover methods fail to reproduce converged canonical distributions. In this respect the method is similar in spirit to the method of Nosé-Hoover chains, but is both more general and Hamiltonian in structure (which allows for the use of efficient sympletic integration schemes). In particular we show the that, within the Generalized Nosé formalism outline herein, any Hamiltonian system can be thermostatted with any other, including a copy of itself. This gives one enormous flexibility in choosing the form of the thermostatting bath. Numerical experiments are included in which a harmonic oscillator is thermostatted with a collection of non-interacting harmonic oscillators as well as by a soft billiard system.

I. INTRODUCTION

The use of extended dynamical systems to generate trajectories with phase points distributed according to a canonical (isothermal) distribution, as opposed to the microcanonical (isoenergetic) distribution generated by traditional Hamiltonian dyanamics, has become standard in molecular dynamics simulation. Of the available approaches, those based on the extended Hamilitonian of Nosé are the most widely used. In this method, the Hamiltonian of the system is augmented by the addition of auxilliary dynamical variables, so that constant energy dynamics in the extended phase space generates a canonical distribution in the reduced phase space of the original system, assuming ergodicity. Although this method is popular, it exhibits limitations when applied to large scale systems with complex chemical structure, such as protein-bath models and quantum-classical systems for which a variety of dynamical components are present in the solution. These limitations are a direct result of simplicity of the Nosé method (which is also one of its most desirable features) and they are only partly ameliorated by the introduction of various devices such as Nosé chains. In this article we show how Nosé's approach can be generalized to incorporate a wide range of bath systems, offering many interesting avenues for improved dynamic sampling. We also demonstrate the construction of efficient numerical methods for this system.

Following the original papers of Nosé[1,2], many modifications of the basic formulation have been proposed. Nosé dynamics accomplishes thermostatting by a dynamic (and artificial) modification of the time-scale. In Reference 3, time and coordinate transformations are introduced to correct the time-scale problem; the resulting Nosé-Hoover dynamics is non-Hamiltonian, although a conserved energy function does exist. The lack of Hamiltonian structure precludes the use of symplectic numerical integration schemes, which have been shown to yield superior long term stability[3], and the design of algorithms for this system has focused on the development of time reversible methods[4]. In an alternative approach[5,6], a Poincaré time transformation is applied to the Nosé Hamiltonian, yielding a new Hamiltonian, which generates canonically distributed dynamics directly in real time. Although the exact phase-space trajectories for the Nosé-Hoover and Nosé-Poincaré methods can easily shown to be identical, the Nosé-Poincaré dynamics is Hamiltonian, allowing for the design of *symplectic*, time-reversible approximate integrators[5,7]. More recently, an alternative symplectic thermostatting scheme has been proposed based on a reformulation of Nosé dynamics in a separated form (with a constant mass matrix), incorporating an on-the-fly recovery of phase variables at fixed time-steps through interpolation or reweighting[8].

In all of these methods, the production of canonically distributed phase-space trajectories requires the system to be sufficiently ergodic that time and ensemble averages are equal within required accuracy. For the strongly coupled, many-particle systems generally encountered in molecular simulation, the dynamics is often sufficiently chaotic for this condition to be met. However, for certain important low dimensional systems (such as the 1-d oscillators[9]) or for many-particle systems with weakly coupled low-dimensional subspaces (such as molecular systems with stiff intramolecular vibrations[10]) the addition of only two auxilliary Nosé variables is not enough to yield sufficiently ergodic phase-space trajectories. To remedy this a number of methods have been proposed that either modify the coupling of the auxilliary variables in the Nosé-Hoover equations of state[11–14], add additional auxilliary variables as in the method of Nosé-Hoover chains[15] For a molecular system with periodic boundary conditions the latter approch has proven to be the more generally useful one. All of these methods to enhance ergodicity, like the Nosé-Hoover approach from which they derive, are non-Hamilitonian in structure and cannot take advantage of symplectic integration schemes.

In this paper, we outline a general method for improving the ergodicity of the Nosé thermostat that is fully Hamilitonian in structure. The method is generated by the introduction of additional auxilliary variables to the Nosé-Poincaré thermostat, in much the same way as the Nosé-Hoover chains are generated from the Nosé-Hoover equations of motion. However, instead of specifically adopting a chain-like coupling for this Extended Nosé-Poincare Hamiltonian, we determine a general form for the coupling, from which an infinitei variety of specific methods can be extracted. This general form is presented in Section III, following a background discussion of the mathematical formulation of Nosé based thermostats in Section II. In Section IV, specific examples of Generalized

Nosé-Poincaré thermostats are introduced and analyzed with numerical experiments.

II. BACKGROUND: THE NOSÉ AND NOSÉ-POINCARÉ HAMILTONIANS

For a system of N particles in d dimensions, the original Nosé Hamiltonian is given by

$$\mathcal{H}_\mathcal{N} = \frac{\tilde{\mathbf{p}}^T \mathbf{M}^{-1} \tilde{\mathbf{p}}}{2s^2} + U(\mathbf{q}) + \frac{\pi_s^2}{2Q_s} + gkT \ln s, \tag{1}$$

where $\mathbf{q}$ and $\tilde{\mathbf{p}}$ are the dN dimension atomic position and conjugate Nosé momentum vectors, respectively, and the scalars s and π_s are auxilliary conjugate position and momentum variables. The Nosé dynamics controls the temperature of the system by rescaling time so that the real time t of the system is related to the Nosé time τ by $\frac{dt}{d\tau} = s$. In addition, the momentum $\mathbf{p}$ of the original system is related to the Nosé momentum by $\mathbf{p} = \tilde{\mathbf{p}}/s$.

The equations of motion for this system are

$$\frac{\mathbf{q}}{d\tau} = \mathbf{M}^{-1}\mathbf{p}/s \tag{2a}$$

$$\frac{d\tilde{\mathbf{p}}}{d\tau} = -\nabla V(\mathbf{q}) \tag{2b}$$

$$\frac{s}{d\tau} = \frac{\pi_s}{Q_s} \tag{2c}$$

$$\frac{\pi_s}{d\tau} = \tilde{\mathbf{p}}^T \mathbf{M}^{-1} \tilde{\mathbf{p}}/s^3 - gkT/s \tag{2d}$$

$$\tag{2e}$$

The Nosé-Hoover equations of motion[15] are generated by transforming the time derivatives to real time, transforming to real momentum and making the coordinate transformations $\eta = \ln s$ and $\xi = \dot{\eta}$. These coordinate and time transformations destroy the canonical Hamiltonian structure of the equations, although there is a conserverd energy function.

As an alternative to Nosé-Hoover, the Nosé-Poincare thermostat[5], a fully Hamiltonian real-time implementation of the Nosé thermostat, is obtained by applying a time transformation directly to the Nosé Hamiltonian as opposed to the equations of motion. The resulting transformed Hamiltonian is given by

$$H_{NP} = s[H_N - H_N(t=0)] .$$

The Nosé-Poincaré Hamiltonian is nonseparable since the kinetic energy contains the extended "position" variable s. The equations of motion for a general time-independent, non-separable Hamiltonian can be written (for general positions Q and conjugate momenta P)

$$\dot{Q} = G(P,Q)$$
$$\dot{P} = F(P,Q) , \tag{3}$$

where $G(P,Q) = \frac{\partial \mathcal{H}}{\partial P}$ and $F(P,Q) = -\frac{\partial \mathcal{H}}{\partial Q}$. (For a separable Hamiltonian, G is only a function of P and F is only a function of Q.) For such a nonseparable system, standard symplectic splitting methods, such as the Verlet/leapfrog algorithm, are not directly applicable. However, symplectic methods specifically for nonseparable systems have been developed[3]. One simple example that is second-order and time-reversible is the Generalized Leapfrog Algorithm (GLA)

$$P_{n+1/2} = P_n + hF(P_{n+1/2}, Q_n)/2$$
$$Q_{n+1} = Q_n + h[G(P_{n+1/2}, Q_n) + G(P_{n+1/2}, Q_{n+1})]/2$$
$$P_{n+1} = P_{n+1/2} + hF(P_{n+1/2}, Q_{n+1})/2 , \tag{4}$$

where h is the time step and P_n and Q_n are the approximations to $P(t)$ and $Q(t)$ at $t = t_n = nh$. This method is a simple example of a class of symplectic integrators for nonseparable Hamiltonians[16–19]. Applying the GLA to the Nosé-Poincaré system gives a numerical method that is semi-explicit (requiring only one force evaluation per timestep), symplectic and time reversible.

The Nos'e-Poincaré method is shown[5] to provide canonical sampling by an argument demonstrating that the microcanonical distributon function in the extended phase space

$$\rho_{MC}(\mathbf{q}, \mathbf{p}, s, \pi_s; N, V, E_N) = \frac{1}{Z_{MC}} \delta\{s[H_N(\mathbf{q}, \mathbf{p}, s, \pi_s) - E_N]\} \tag{5}$$

(where Z_{MC} is the microcanonical partition function obtained by integrating ρ_{MC} over the extended phase space) generates a canonical distribution in the reduced phase space. The proof relies on simply performing the integrations with respect to the auxiliary variables.

III.   A GENERALIZED EXTENDED NOSÉ THERMOSTAT

In this section we show that the Nosé approach (and its corresponding real-time version - Nosé-Poincare) is only the simplest realization of a vast range of generalized thermostatting Hamiltonians. In particular, we show below that canonical sampling can be achieved as well if the Nosé Hamiltonian is coupled to an auxillary system (with position variables $\{\sigma_i\}$ and conjugate momenta $\{\pi_i\}$) to generate a Generalized Nosé Hamiltonian

$$H_{GN} = H(\mathbf{q}, \tilde{\mathbf{p}}/s) + gkT \ln s + f(\pi_s, \sigma_i, \pi_i) , \tag{6}$$

where H is the Hamiltonian for the original system to be thermostated, s and π_s are the usual Nosé thermostat variables and f is a continous function that must be chosen so that it is bounded below and so that $exp(-\beta f)$ is in L_1 on its domain, i.e. so that its absolute integral is finite. The corresponding real-time Generalized Nosé-Poincaré Hamiltonian is then

$$H_{GNP} = s[H_{GN} - H_{GN}(t = 0)] . \tag{7}$$

The proof that this Generalized Nosé-Poincaré generates a canonical distribution (assuming ergodicity) follows closely that for the standard Nosé-Poincareé approach[5] and is given here for completeness. The statistical distribution for the reduced set of variables, $\mathcal{P}(\mathbf{p}, \mathbf{q})$ is given by an integral over the extended variable distribution $\mathcal{P}_{ext}(\mathbf{p}, \mathbf{q}, s, \boldsymbol{\Lambda})$ (where $\boldsymbol{\Lambda}$ denotes the vector of auxilliary variables $(\pi_s, \{\sigma_i\}, \{\pi_i\})$):

$$d\mathbf{q} \, d\mathbf{p} \, \mathcal{P}(\mathbf{p}, \mathbf{q}) = \int d\mathbf{q} \, d\tilde{\mathbf{p}} ds d\boldsymbol{\Lambda} \mathcal{P}_{ext}(\mathbf{p}, \mathbf{q}, s, \boldsymbol{\Lambda}) , \tag{8}$$

where the integral is over the auxiliary variables s and $\boldsymbol{\Lambda}$. Assuming that the dynamics is ergodic,

$$d\mathbf{q} \, d\mathbf{p}\mathcal{P}(\mathbf{p}, \mathbf{q}) = \frac{1}{Z_{GN}N!h^{N_f}} \int ds \int d\boldsymbol{\Lambda} \, d\tilde{\mathbf{p}} \, d\mathbf{q} \, \delta\{s[H(\mathbf{p}/s, \mathbf{q}) + \tag{9}$$
$$+ gkT \ln s + f(\boldsymbol{\Lambda}) - H_{GN}(0)]\} ,$$

where Z_{GNP} represents the partition function for the Generalized Nosé-Poincaré Hamiltonian and N_f is the number of degrees of freedom in the thermostatted system. Changing variables to real momenta $\mathbf{p} = \tilde{\mathbf{p}}/s$ gives

$$d\mathbf{q} \, d\mathbf{p} \, \mathcal{P}(\mathbf{p}, \mathbf{q}) = \frac{d\mathbf{p} \, d\mathbf{q}}{Z_{GN}N!h^{N_f}} \int ds \, d\boldsymbol{\Gamma} \, s^{N_f} \delta\{s[H(\mathbf{p}, \mathbf{q}) + gkT \ln s + f(\boldsymbol{\Gamma}) - H_{GN}(0)]\} \tag{10}$$

4

For a function $\phi(s)$ with a single pole at $s = s_0$ we have

$$\delta(\phi(s)) = \frac{\delta(s - s_0)}{|\phi'(s_0)|} \, ,$$

which, for our case, gives

$$dq\,dp\,\mathcal{P}(\mathbf{p}, \mathbf{q}) = \frac{d\mathbf{p}\,d\mathbf{q}}{Z_{GN}N!h^{N_f}} \int ds \int d\mathbf{\Lambda}\, \frac{s^{N_f}}{gkT}\delta\{s - \exp\left[-\frac{1}{gkT}(H(\mathbf{p}, \mathbf{q})\right. \tag{11}$$
$$\left. +f(\mathbf{\Lambda}) - H_{GN}(0)]\}\right.$$

Integration over s yields

$$dq\,d\mathbf{p}\mathcal{P}(\mathbf{p}, \mathbf{q}) = \frac{d\mathbf{q}\,d\mathbf{p}}{gkTZ_{GN}N!h^{N_f}} \int d\mathbf{\Lambda}\, \exp\left[-\frac{N_f}{gkT}(H(\mathbf{p}, \mathbf{q})\right. \tag{12}$$
$$\left. +f(\mathbf{\Lambda}) - H_{GN}(0)]\}\right.$$

Setting $g = N_f$ and integrating over the remaining auxilliary variables, $\mathbf{\Lambda}$ gives

$$\mathcal{P}(\mathbf{p}, \mathbf{q}) = \frac{C}{Z_{GN}N!h^{N_f}} \exp\left[-\beta H(\mathbf{p}, \mathbf{q})\right] , \tag{13}$$

where $\beta = (kT)^{-1}$ and we have assumed certain properties of the function $f(\mathbf{\Lambda})$ to insure that the integration converges, namely,

- f is bounded below

- $exp-\beta f \in L_1$.

Applying the same proceedure to Z_{GN} and canceling constants gives

$$\mathcal{P}(\mathbf{p}, \mathbf{q}) = \frac{1}{ZN!h^{N_f}} \exp\left\{-\beta[H(\mathbf{p}, \mathbf{q})]\right\} , \tag{14}$$

which is the usual canonical distribution, with Z being the standard canonical partiion function.

$$Z = \frac{1}{N!h^{N_f}} \int d\mathbf{p} \int d\mathbf{q} \exp\left\{-\beta[H(\mathbf{p}, \mathbf{q})]\right\} . \tag{15}$$

(It should be noted that in the original Nosé-Poincaré paper[5], a method for Nosé-Poincaré chains was outlined; however, this method violates the conditions on f given above and is invalid.)

A useful subclass of Generalized Nosé Hamiltonians can be generated by viewing the standard Nosé Hamiltonian as the "system" and the auxillary variable $\{\sigma_i, \pi_i\}$ as a "bath" giving

$$H_{GN} = H_N(\tilde{\mathbf{p}}, \mathbf{q}, s, \pi_s) + H_{\text{bath}}(\{\sigma_i, \pi_i\}) + H_{\text{int}}(\pi_s, \{\sigma_i, \pi_i\}) \tag{16}$$

where H_N is the usual Nosé Hamiltonian and the system-bath interaction Hamiltonian, H_{int}, has no dependence on s to preserve the canonical distribution, but is otherwise arbitrary (within the constraints on f outlined above). This gives us the result that a given Hamiltonian system can be thermostated by coupling it to any other system, including a copy of itself!

For such a broad class of Generalized Hamiltonians it is not possible to give a general numerical discretization scheme that is optimal for all members of the class, but for any given specific case, efficient schemes can be devised. In the next section we give two specific examples of Generalized Nosé-Poincaré systems and outline efficient, symplectic numerical integration algorithms for each.

IV. EXAMPLE GENERALIZED NOSÉ-POINCARÉ THERMOSTATS: ALGORITHMS AND NUMERICAL EXPERIMENTS

In this section, two examples of Generalized Nosé-Poincaré thermostats are presented along with appropriate symplectic numerical discretization schemes. In addition, numerical experiments are performed to show that these methods can successfully thermostat a 1-d harmonic oscillator. Note that, these are merely intended as representative examples of the infinite set of possible generalized thermostats and are in no sense being touted as optimal.

A.   Example 1: 'vertex' coupling to independent harmonic oscillators

Consider the following specific Generalized Nosé Hamiltonian

$$\mathcal{H}_{\mathcal{GN}} = \frac{\tilde{\mathbf{p}}^T \mathbf{M}^{-1} \mathbf{p}}{2s^2} + V(\mathbf{q}) + gkT\ln s + \frac{(1+\sum \sigma_i^2)\pi_s^2}{2Q_s} + \sum_i \frac{\sigma_i^2}{2} + \sum_{i=1,m} \frac{\pi_i^2}{2Q_i} \tag{17}$$

We refer to this model as a 'vertex' coupling as the σ_i are only coupled to the other variables through π_s (a common vertex). The Generalized Nosé-Poincaré Hamilitonian for this system is generated in the usual way

$$H_{GNP} = s[H_{GN} - H_{GN}(t=0)]. \tag{18}$$

The equations of motion for this example Generalized Nosé-Poincaré system are

$$\dot{\tilde{\mathbf{p}}} = -s\nabla V(\mathbf{q}) \tag{19a}$$

$$\dot{\mathbf{q}} = \mathbf{M}^{-1}\tilde{\mathbf{p}}/s \tag{19b}$$

$$\dot{s} = \frac{s(1+\sum \sigma_i^2)\pi_s}{Q_s} \tag{19c}$$

$$\dot{\pi}_s = \tilde{\mathbf{p}}^T \mathbf{M}^{-1}\tilde{\mathbf{p}}/s^2 - gkT - [H_{GN} - H_{GN}(t=0)] \tag{19d}$$

$$\dot{\sigma}_i = \frac{s\pi_i}{Q_i} \tag{19e}$$

$$\dot{\pi}_i = -s(1+\pi_s/Q_s)\sigma_i \tag{19f}$$

To generate a symplectic integration scheme, often the best approach is to use a splitting method in which the Hamiltonian is written as the sum of simpler Hamiltonians for which the equations of motion can be intergrated either exactly or with known simple symplectic schemes[3]. The overall discretization scheme is then given as the concatenation of those for the subproblems. For this Vertex Generalized Nosé-Poincaré, the following splitting can be used:

$$H_1 = -s\left[\frac{(1+\sum \sigma_i^2)\pi_s^2}{2Q_s} + \frac{1}{2}\sum_i \sigma_i^2 + gkT\ln s\right] \tag{20}$$

$$H_2 = s\left[\frac{\tilde{\mathbf{p}}^T \mathbf{M}^{-1}\tilde{\mathbf{p}}}{2s^2} + \sum \frac{\pi_i^2}{2Q_i}\right] \tag{21}$$

$$H_3 = s[V(q) - H_{GNP}(t=0)] \tag{22}$$

This splitting is similar to one proposed by Nosé for the original Nosé-Poincaré method[7]. The numerical method is then generated by the concatination

$$\phi_H(t) = \phi_{H_1}(t/2)\phi_{H_2}(t/2)\phi_{H_3}(t)\phi_{H_2}(t/2)\phi_{H_1}(t/2) + \mathcal{O}(t^3) , \tag{23}$$

6

where $\phi_H(t)$ is the solution map that advances a phase space point forward in time by t under the dynamics defined by Hamiltonian H. The solution maps for H_2 and H_3 can be performed exactly and that for H_1 can be approximated using the Generalized Leap-Frog Algorithm (GLA) discussed in Section II to yield a second-order method that is both time reversible and symplectic.

B.   Example 2: Coupling to a "realistic" system: the 3 soft-particle bath

A standard example of a system that is provably ergodic is the 3-ball billiard system consisting of three hard-sphere particles moving in a box with hard boundaries. While we could, in principle, develop numerical schemes for handling a hard-sphere bath, using the technique described in Reference[20], this would be quite complicated. Instead, we use a simplified bath consisting of 3 soft repulsive spheres constrained to a small regiion via a harmonic tether to the origin. While we are aware of no proof that this system is ergodic, we will assume that is for the purposes of this demonstration. Using the system/bath notation in Eq. 16 the bath and interaction Hamiltonians for this system are given by

$$H_{\text{bath}} = \sum_{i=1}^{3} \frac{\mid \pi_i \mid^2}{2Q_i} + \sum_{i=1}^{3} \frac{\mid \sigma_\mathbf{i} \mid^2}{2} + \sum_i \sum_{j>i} \mid \sigma_\mathbf{i} - \sigma_\mathbf{j} \mid^{-12} \tag{24}$$

and

$$H_{\text{int}} = \left(\sum_{i=1}^{3} \mid \sigma_i \mid^2 \right) \frac{\mid \pi_s \mid^2}{2Q_s} . \tag{25}$$

Here the bath positions and momenta σ_i and π_i are vectors in $\mathcal{R}^3$. The Nosé-Poincaré equations for this system can be integrated using a similar Hamiltonian splitting to that used in the vertex coupling

$$
\begin{aligned}
H_1 &= s[gkT \ln s + (\sum_{i=1,3} \mid \sigma_i \mid^2) \left(1 + \frac{\pi_s^2}{2Q_s} \right) \\
H_2 &= s \left[\frac{\mathbf{p}^T \mathbf{M}^{-1} \mathbf{p}}{2s^2} + \sum_{i=1}^{3} \frac{\mid \pi_i \mid^2}{2Q_i} \right] \\
H_3 &= s[V(\mathbf{q}) - H_{GN}(t = 0)] .
\end{aligned}
\tag{26}
$$

The dynamics for H_2 and H_2 can be integrated exactly and that for H_1 can be integrated using the GLA discussed in Section II.

C.   Numerical Experiments

We apply the two Generalized Nosé-Poincaré Hamiltonians above to the problem of thermostatting a 1-d harmonic oscillator. This system exhibits quite severe deviations from ergodicity for the unaugmentent Nosé thermostats[15], which is the main reason for the difficulty encountered in thermostatting molecular systems with stiff bonds that are weakly coupled to the rest of the system[10]. The unthermostatted Hamiltonian for this system is

$$H(p, q) = \frac{p^2}{2} + \frac{q^2}{2}$$

where we have assume unit mass and radial frequency.

To test the sampling we have performed MD simulations at $kT = 1.0$ on this model using both the vertex coupling (with $Q_s = 1.0$ and 5 auxilliary variables with masses Q_i equal to 0.7, 0.9, 1.2, 1.8 and 2.8) and the three-sphere coupling (with $Q_s = 1.0$ and all sphere masses set to 2.0). In Fig. 1 are shown the results for the distribution of q for both couplings in runs of $2{\times}10^6$ steps with a time step $h = 0.005$. The solid line in Fig. 1 shows, for comparison, the exact canonical distribution for this system at the target temperature. In all cases the energy error was less than $1{\times}10^{-4}$ with no discernable energy drift.

V. CONCLUSIONS

We have demonstrated that the Nosé[1,2] and Nosé-Poincaré[5] methods for constant-temperature molecular-dynamics simulation can be substantially generalized by the addition of auxilliary variables to encompass an infinite variety of Hamiltonian thermostats. Such themostats can be used to enhance ergodicity in systems, such as the 1-d harmonic oscillator[9] or certain molecular systems[10], for which the standard Nosé-Hoover[9] and Nosé-Poincaré methods fail to reproduce converged cannonical distributions. The addition of additional variables to an extended Hamiltonian system is much in the spirit of previous work to improve the convergence of the non-Hamiltonian Nos'e-Hoover thermostat, namely, through the use of Nosé-Hoover chains[15] or Gaussian Thermostatting[14], but the methods described in this work are far more general and are fully Hamiltonian in form, which allows for the use of symplectic integration schemes, which have been shown to have superior stability in long simulations[3].

In particular we demonstrate the remarkable result that, within the Generalized Nosé formalism outline herein, any Hamiltonian system can be thermostatted with any other, including a copy of itself. This gives one enormous flexibility in choosing the form of the thermostatting bath. For example, one could use as the thermostatting bath system a collection of coupled oscillators with natural frequencies that mimic those in the system to be thermostatted allowing for more efficient energy transfer from system to bath. In this Multiresonant Nosé approach, the bath frequencies and couplings could be tuned for optimal performance. In another approach, one could use as the thermostatting system a subset of the full system; for example, one could thermostat a system of biomolecules in solution with a small sample of water at the desired temperature. It is clear that further study is needed to understand how one constructs an optimal thermostatting bath for a given system. The Generalized Nosé approach provides a useful general framework within which such investigations can be undertaken in a systematic way.

[1] S. Nosé, Mol. Phys. **52**, 255 (1984).

[2] S. Nosé, J. Chem. Phys. **81**, 511 (1984).

[3] J.M. Sanz-Serna and M.P Calvo, *Numerical Hamiltonian Problems*, (Chapman and Hall, New York, 1995).

[4] G.J. Martyna, M.E. Tuckerman, D.J. Tobias, and M.L. Klein, Mol. Phys. **87**, 1117 (1996).

[5] S.D. Bond, B.J. Leimkuhler, and B.B. Laird, J. Comp. Phys. **151**, 114 (1999).

[6] C.P. Dettmann and G.P. Morriss, Phys. Rev. E **54**, 2495 (1996).

[7] S. Nose, J. Phys. Soc. Japan **70**, 75 (2001).

[8] B.J. Leimkuhler, Comp. Phys. Comm. **148**, 206 (2002).

[9] W.G. Hoover, Phys. Rev. A **31**, 1695 (1985).

[10] S. Toxværd, Ber. Bunsenges. Phys. Chem **94**, 274 (1990).

[11] I.P. Hamilton, Phys. Rev. A **42**, 7467 (1990).

[12] D. Kusnezov, A. Bulgac, and W. Bauer, Ann. Phys. **204**, 155 (1990).

[13] R.G Winkler, Phys. Rev. A **45**, 2250 (1992).

[14] Y.Liu and M.E. Tuckerman, J. Chem. Phys. **112**, 1685 (2000).

[15] G.J. Martyna, M.L. Klein, and M. Tuckermann, J. Chem. Phys. **97**, 2635 (1992).

[16] J.M. Sanz-Serna, BIT **28**, 877 (1991).

[17] F. Lasagni, Zeit. Angew. Math. Phys. **39**, 952 (1988).

[18] Y.B. Suris, U.S.S.R. Comput. Maths. Math. Phys. **29**, 138 (1989).

[19] J.M. Sanz-Serna, Acta Numer. **1**, 243 (1991).

[20] Y.A. Hounonougbo, B.B. Laird, and B.J. Leimkuhler, Mol. Phys. **98**, 309 (1999).

FIGURE CAPTION

FIGURE 1: The probability distribution for the position q of a harmonic oscillator thermostatted at $kT = 1.0$ by the Generalized Nosé-Poincaré vertex (squares) and three-sphere (circles) couplings discussed in Section IV. Specific parameters used for each simulation are given in the text. For comparison, the exact canonical distribution expected is shown as a solid line.
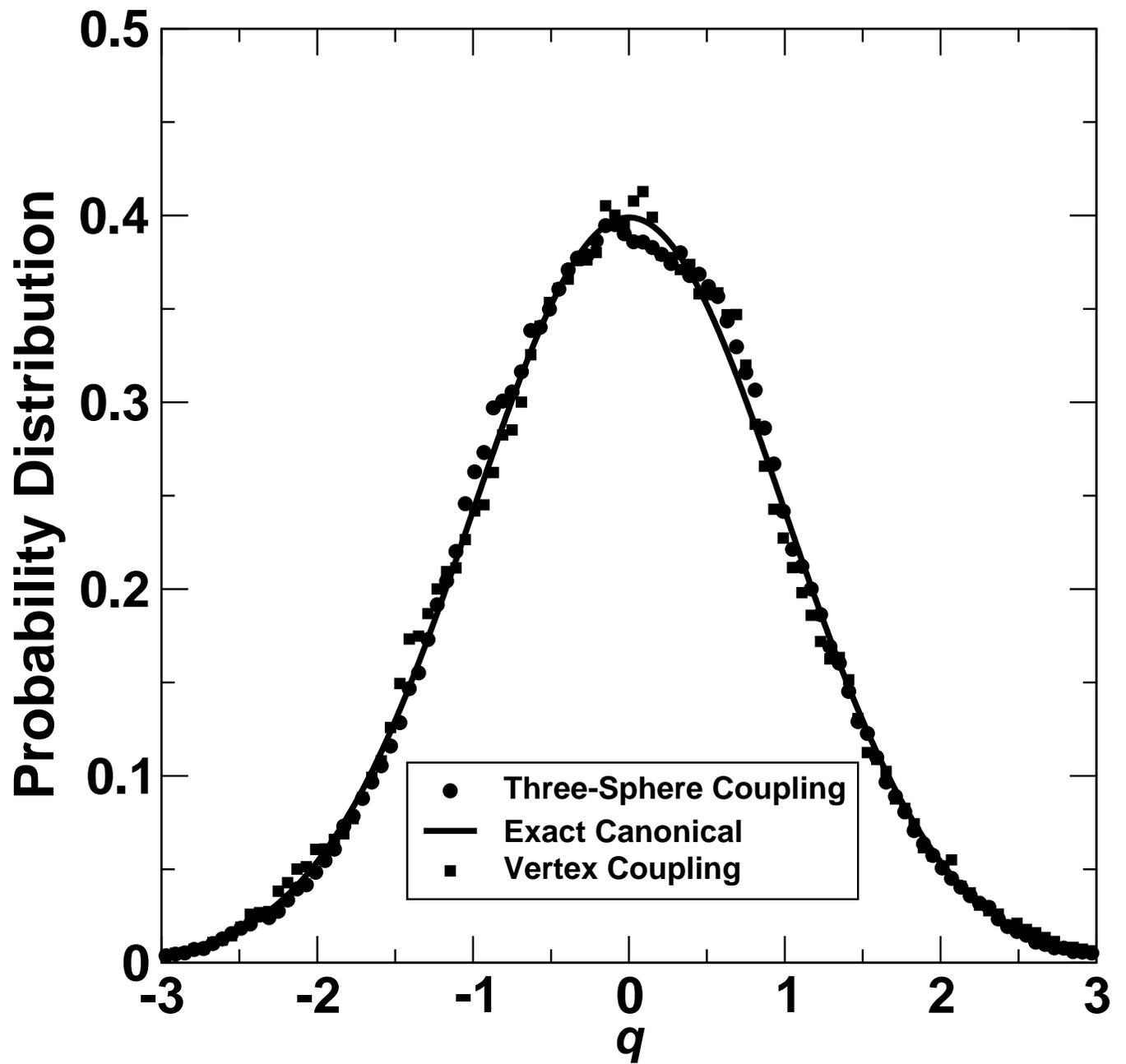
FIG. 1: